Infection of lung megakaryocytes and platelets by SARS-CoV-2 anticipate fatal COVID-19

Aiwei Zhu, Fernando Real, Claude Capron, Arielle R Rosenberg, Aymeric Silvin, Garett Dunsmore, Jaja Zhu, Andréa Cottoignies-Callamarte, Jean-Marc Massé, Pierre Moine, et al.

Infection of lung megakaryocytes and platelets by SARS-CoV-2 anticipate fatal COVID-19

Aiwei Zhu[1,2,3,ʃ], Fernando Real[1,2,3,ʃ], Claude Capron[4], Arielle R. Rosenberg[1,2,3,5], Aymeric Silvin[6], Garett Dunsmore[6], Jaja Zhu[4], Andréa Cottoignies-Callamarte[1,2,3], Jean-Marc Massé [2,3,7], Pierre Moine[8], Simon Bessis[8], Mathieu Godement[8], Guillaume Geri[9,10], Jean-Daniel Chiche[11], Silvana Valdebenito[12], Sandrine Belouzard[13], Jean Dubuisson[13], Geoffroy Lorin de la Grandmaison[14], Sylvie Chevret[15], Florent Ginhoux[16], Eliseo A Eugenin[12], Djillali Annane[8], Elisabeth Cramer Bordé[1,2,4,10], Morgane Bomsel[1,2,3*]

[1] Mucosal Entry of HIV and Mucosal Immunity, Institut Cochin, Paris-Descartes University, Paris, France.
[2] INSERM U1016.
[3] CNRS UMR8104.
[4]Service d'Hématologie Hôpital Ambroise Paré (AP-HP), Boulogne-Billancourt, France.
[5]Hôpital Cochin, Service de Virologie, Hôpital Cochin (AP-HP), Paris, France.
[6]INSERM U1015, Gustave Roussy Cancer Campus, Villejuif, France.
[7] Electron Microscopy plateform, Institut Cochin, Paris-Descartes University, Paris, France.
[8] FHU SEPSIS (Saclay and Paris Seine Nord Endeavour to PerSonalize Interventions for Sepsis), RHU RECORDS (Rapid rEcognition of CORticosteroiD resistant or sensitive Sepsis), Department of Intensive Care, Hôpital Raymond Poincaré (APHP), Laboratory of Infection & Inflammation – U1173, School of Medicine Simone Veil, University Versailles Saint Quentin – University Paris Saclay, INSERM, Garches, France.
[9] Service de Réanimation, Hôpital Ambroise Paré (AP-HP), Boulogne-Billancourt, France.
[10] Université de Versailles-St Quentin en Yvelines, France.
[11] Service de Réanimation, Hôpital Cochin (AP-HP), Paris, France.
[12] Department of Neuroscience and Cell Biology, University of Texas Medical Branch (UTMB), Galveston, Texas, 77553, USA.
[13] Virologie moléculaire et cellulaire des coronavirus, Centre d'infection et d'immunité de Lille, Institut Pasteur de Lille, Université de Lille, CNRS, Inserm, CHRU, 59000 Lille, France.
[14] Service d'Anatomie et cytologie pathologiques - Médecine légale, Hôpital Raymond Poincaré (AP-HP), Garches, France.
[15]Service de Biostatistique, Hôpital Saint Louis (AP-HP), Paris, France.
[16]Singapore Immunology Network (SIgN), Agency for Science, Technology and Research (A(∗)STAR), Biopolis, Singapore; Shanghai Institute of Immunology, Shanghai JiaoTong University School of Medicine, Shanghai, China; Translational Immunology Institute, SingHealth Duke-NUS Academic Medical Centre, Singapore.

ʃequal contribution

*Correspondence and Lead contact: MB. morgane.bomsel@inserm.fr
Laboratory of Mucosal Entry of HIV and Mucosal Immunity, Institut Cochin, 75014 Paris, France
Telephone: +33-1-40-51-64-97
Fax: +33-1-40-51-64-54

Keywords: Platelets; SARS-CoV-2; COVID-19; Megakaryocytes; Lung; Macrophages

Short title: Platelets carry infectious SARS-CoV-2 in fatal COVID-19

Abstract

SARS-CoV-2, although not being a circulatory virus, spread from the respiratory tract resulting in multiorgan failures and thrombotic complications, the hallmarks of fatal COVID-19. A convergent contributor could be platelets that beyond hemostatic functions can carry infectious viruses. Here, we profiled 52 patients with severe COVID-19 and demonstrated that circulating platelets of 19 out 20 non-survivor patients contain SARS-CoV-2 in robust correlation with fatal outcome. Platelets containing SARS-CoV-2 might originate from bone marrow and lung megakaryocytes (MKs), the platelet precursors, which were found infected by SARS-CoV-2 in COVID-19 autopsies. Accordingly, MKs undergoing shortened differentiation and expressing anti-viral IFITM1 and 3 RNA as a sign of viral sensing were enriched in the circulation of deadly COVID-19. Infected MKs reach the lung concomitant with a specific MK-related cytokine storm rich in VEGF, PDGF and inflammatory molecules, anticipating fatal outcome. Lung macrophages capture SARS-CoV-2-containing platelets *in vivo*. The virus contained by platelets is infectious as *in vitro* capture of platelets carrying SARS-CoV-2 propagate infection to macrophages in a process blocked by an anti-GPIIbIIIa drug. Altogether, platelets containing infectious SARS-CoV-2 inflect COVID-19 pathogenesis and provide a powerful fatality marker. Clinical targeting of platelets might prevent viral spread, thrombus formation and exacerbated inflammation at once and increase survival in COVID-19.

Introduction

Since December 2019, the world has experienced an outbreak of coronavirus disease 2019 (COVID-19), caused by the severe acute respiratory syndrome coronavirus 2 (SARS-CoV-2). Although the epidemiological and clinical characteristics of patients with COVID-19 have been reported, biological risk factors for mortality are needed. Critical cardio-vascular, as well as multifactorial thrombotic complications in patients with COVID-19 are frequent, even in individuals without a history of cardio-vascular disease (1). Furthermore, patients with severe COVID-19 admitted into intensive care unit (ICU) have increased cumulative thrombotic complications compared with patients not admitted to ICU (31% versus 1.3%) (2). Microthrombotic events are especially frequent in the lungs where MKs, the platelet precursors, are found to accumulate atypically in COVID-19 patients (3), suggesting abnormal behaviour (4). However anticoagulant treatment of COVID-19 patients is of limited efficacy, and any benefit may be patient-specific (5, 6). Despite clinical evidence of a link between COVID-19 and haemostatic disorders, the underlying mechanisms of thrombosis remain uncertain.

The β-coronavirus SARS-CoV-2 is a single strand RNA (+) enveloped virus (7). The viral spike protein-1 binds to its main receptors, the surface expressed angiotensin-converting enzyme-2 (ACE-2) and TMPRSS2 (8), through which the virus infects target cells. Virus replication involves the production of double-stranded (positive- (+)/negative- (-) strand) complexes in the cytosol of the infected cells initiating viral component production. SARS-CoV-2 infected cells are found not only in the lung, but the virus is also widely found in other tissues (9). The means of viral dissemination remains unknown. Since there is a lack of significant blood viremia, but only occasional detection of viral RNA, since blood cells are rarely infected (10-12), and since no studies have so far demonstrated the presence of viruses and their infectiousness, our results indicate that the major route of SARS-CoV-2 dissemination is not blood.

Platelets have a critical role in hemostasis and thrombosis (13). Their interaction with the subendothelium during viral infection results in platelet hyperactivity and in turn, arterial thrombus producing end-organ ischemia. In particular, the influenza virus can directly activate platelets (14, 15) with consequent uncontrolled coagulation cascade resulting in lung injury. Besides their role in hemostasis, platelets have immunological function contributing to the immune response and inflammation (13, 16, 17). Platelets can also harbor pathogens including viruses (18, 19) where some, such as Dengue virus, may even replicate (20). Furthermore, HIV as well as Dengue and influenza virus can infect MKs (21), the cell producing platelets (21-23). Accordingly, platelets can also shelter viruses such as HIV *in vivo* as we have recently shown (22), thereby participating in the propagation of the infection and altering the viral pathology. Platelets are hyperactivated in COVID-19 and transcriptomics found N and more often E genes associated with platelets in some patients irrespective of disease severity (24, 25). Whether MK infection occurs and replication-competent SARS-CoV-2 is contained in platelets with a possible role in both COVID-19 thrombophilia and virus spread have not been addressed.

Material and Methods

Patients and ethical statement

This non-interventional study was approved by the institutional review board of the ethical committee for research (CER) of the University of Paris-Saclay (CER-Paris-Saclay-2020-050) and conformed to the principles outlined in the Declaration of Helsinki. Accordingly, all participants were informed in writing about the study and allowed not to participate. We studied prospectively samples from 76 COVID-19 patients admitted at the Cochin (Paris, France), Ambroise Paré (Boulogne-Billancourt, France), and Raymond Poincaré (Garches, France) Hospitals between March and May 2020. All patients had COVID-19 diagnosis confirmed by SARS-CoV-2 RNA RT-qPCR in nasopharyngeal swabs at the hospital. For this study, blood (n= 52), bronchoalveolar lavages (BAL) (n=19) and autopsy (n=5) unpaired samples were obtained from severe COVID-19 patients.

Additional methods are detailed in supplementary material.

Results

Platelets from COVID-19 non-survivors harbor SARS-CoV-2

Platelet samples from randomly chosen individuals with confirmed severe COVID-19 diagnosis (n=30) (Figure S1, Table 1, S1-2) were screened for SARS-CoV-2 by RT-qPCR (ORF, S and N genes). SARS-CoV-2 RNA was detected in 7 out of 30 patients. Strikingly, 6 out of the 7 platelet positive patients died within the week following sampling (mean days [95%CI]: 8.3 [5-14]), thus referred as non-survivors. Among the group of surviving patients (survivors), only 1 out of 24 platelet samples contained the viral RNA (Figure 1A, mean [95%CI] RNA copies/million platelets in samples from non-survivors versus survivors, for ORF1 gene: 580 [160-1200] vs 2.2 [1.8-8.2], $p<0.001$; for S gene: 840 [160-1600] vs 1.3 [1.1-5], $p<0.001$; for N gene: 1200 [320-2000] vs 1.6 [1.3-5.6], $p<0.001$). Using 11 of these samples and additional ones from 28 patients, we then evaluated if the RNA detected in platelets corresponded to full viral particles, using a flow cytometry technique for combined detection of SARS-CoV-2 RNA and spike proteins in platelets, referred to as FISH-Flow (22) we now validated for SARS-CoV-2 (Figure S2 and Table S3). Detection of both viral RNA and protein was remarkably more frequent in platelets from non-survivors than from survivors (Figure 1B, Figure S2, mean % [95%CI] of $RNA^+/spike^+$ platelets in samples from non-survivors versus survivors, 0.22 [0.06-0.42] vs 0.02 [0.01-0.07], $p=0.001$).

Taken RT-qPCR and FISH-Flow analyses together, SARS-CoV-2 virus was detected within circulating platelets in 20 patients out of 52, from which 19 died (Figure 1C) in direct correlation with fatal outcome that persisted after adjustment for age (OR 63.4 [95% CI 6.6 to 610.1], $p=0.0003$). Of note, the time from first symptoms to sampling was similar between survivors and non-survivors with mean value of 10 days [95% CI 6;26] and 7 [95% CI 5;12.5], respectively (p=0.22), and thus did not introduce a bias in the analysis. The presence of SARS-CoV-2 in platelets was the strongest factor associated with fatal outcome with $p < 0.0001$ in a multivariate analysis based on all patients' clinical data collected (Table 1).

In non-survivor patients, the virus resided inside platelets and was not associated to platelet surface: this was demonstrated by confocal microscopy after viral (+) and (-) strands RNA *in situ* hybridization using RNAscope technology (22) we validated (Figure S3A), coupled to immunostaining of the platelet marker

CD41 (Figure 1D-E and Figure S3B-C). In contrast, no viral signal was found in platelets from survivors. At the ultrastructural level, spherical crowned structures with a diameter of 50-80nm and visible spikes at their periphery typical of SARS-CoV-2 (26-30) were detected inside non-survivor platelets (Figure 1F and Figure S3D). These viral structures were found in subcompartments of the open canalicular system (OCS) (31) as well as in another type of compartment similar to the intra-platelet localization of dengue virus (32), whereas HIV (22), and Influenza viruses (33) are exclusively found in the lumen of OCS. Immunolabeling of SARS-CoV-2 spike proteins on cryosections from these non-survivor platelets (Figure 1G and Figure S3E) confirmed the SARS-CoV-2 nature of the viral spherical crowned images observed above (Figure 1F and Figure S3D). Immunolabeled viruses were again exclusively detected within platelets, with no virus detected at the platelet surface. No such crowned viral structures nor immunolabelling were observed in survivor platelets. Platelets from non-survivors appeared also hyperactivated as indicated by the increase in frequency of platelets surface stained with Von Willebrand factor (vWF) in non-survivors versus survivors or healthy donors (Figure S4A-B) (34).

Although SARS-CoV-2 genes are scarcely found in blood (10, 11, 35), viral genes were more frequently detected in plasma (here in platelet-poor plasma (PPP)) from non-survivors than survivors (66% vs 25%) (Figure S4C). Furthermore, viral RNA copy number detected per million platelets in PRP was not proportional to that detected per ml of PPP using RT-qPCR (Figure S4D), indicating that viral genes detected in the plasma is not the source of virus detected in platelets. In addition, platelets from healthy donor incubated with infectious SARS-CoV-2 were unable to internalize SARS-CoV-2 (Figure S4E-G), confirming that the source of SARS-CoV-2 in patient platelets was not by endocytosis of virus possibly present in the plasma.

In COVID-19 non-survivors, megakaryocytes are produced following a shortened megakaryopoiesis and express viral sensing genes

Alternative to virus endocytosis, platelets could have acquired SARS-CoV-2 in the bone marrow during maturation of their precursors, the megakaryocytes (MKs) that would be infected. This has been observed in Dengue and Influenza virus infection (21). After entering the cava vein, bone marrow MKs reach the pulmonary circulation and then the lung (36). These large MKs are filtrated in the pulmonary capillary bed producing platelets locally but also releasing MKs with monolobed nucleus that are found later on in the peripheral circulation (37, 38). Such monolobed MKs present in PBMCs were thus used as easily accessible surrogates for bone marrow MKs (4, 39). Accordingly, monolobed MKs were detected at low frequencies in PBMCs from non-COVID-19 healthy individuals and COVID-19 survivors but their frequency strikingly increases in COVID-19 non-survivor samples (Figure 2A and Figure S5A).

To further compare MK characteristics in COVID-19 non-survivors versus survivors and healthy controls, we integrated two PBMC single-cell RNA sequencing (scRNA-seq) data sets (4, 39) including healthy donor, COVID-19 survivor and non-survivor samples. Clustering analysis revealed that MK transcriptome profile was more diverse in severe COVID-19 than in healthy controls (Figure 2B-C and Figure S5B-D). Furthermore, genes associated with megakaryopoiesis in severe COVID-19 pointed to a shortened MK differentiation process consistent with the non-classical pathway recently described that bypasses the MK-

erythroid progenitors (MEP) step from the classical differentiation route (40) and associated to inflammatory conditions (41) (Figure 2D and Figure S5E).

Strikingly, when compared with healthy donors and survivors, a unique MK profile (cluster 3) was enriched in non-survivors, both when cells were analyzed altogether (Figure 2B-C) and by individuals (Figure 2E). Resulting differentially expressed genes (DEG) in Cluster 3 (Figure S6A-B) comprised platelet secreted molecules upon activation such as PF4, inflammatory genes such as S100A8, a large set of IFN-stimulated genes (IFI6, IFI27, IFTIM3) that attest viral sensing, and genes driving megakaryopoiesis (PF4, MYL9, and histone associated genes). Accordingly, Cluster 3 specifically associated pathways included not only rapid MK development and platelet functions but also viral sensing by INF-stimulated genes and inflammation (Figure S6B-C). Cluster 3-enriched transcription factors such as JUND, GATA1, and RUNX1 were characteristic of megakaryopoiesis while NFKB1, RELA and STAT3 characterized an inflammatory immune response (Figure S6B). Inferred cluster 3 transcription factors targets were also enriched in IFN regulatory factors (Figure S6B). Among all trajectories rooted on cluster 0 (Figure S6D) predominant in MKs from healthy donors (Figure 2B-C), the one transitioning MKs from cluster 0 to 3 (Figure S6D) confirmed the significant increase of histone-associated and inflammatory genes but also that of antiviral IFN-stimulated genes (Figure 2F).

Infected bone marrow MKs in COVID-19 patients as a source of platelets containing SARS-CoV-2

Altogether, the scRNA-seq results indicated that MKs from COVID-19 non-survivors have matured faster than usual and have sensed the virus, thus being likely infected. In addition, MKs at an abnormally higher density were detected in bone marrow from COVID-19 versus non-COVID-19 autopsy cases (Table 2 and Figure 2G, 49.89±14.37 cells per mm^2 versus 13±3 cells per mm^2, p=0.0001), with an increased diameter size (103.36±42.36 μm versus 30-100 μm). Furthermore, these bone marrow MKs recurrently contained replicative viral (-) RNA (Figure 2H) with 14.99± 9.58 % of the bone marrow MKs positive to (-) SARS-CoV-2 RNA (Figure S7A), establishing that MKs are infected in the bone marrow in COVID-19 non-survivors and constitute the likely source for producing platelets containing SARS-CoV-2.

Infected MKs are retained in the lung in COVID-19 non-survivors

Bronchoalveolar lavages (BAL) from severe COVID-19 patients provide an easily accessible fluid to probe the lung thrombotic and inflammatory environment during the progression of the disease. Thus, among a panel of factors implicated in hemostasis, inflammation and tissue repair analyzed, PF4/CXCL4 (platelet activation) and S100A8 (neutrophil and macrophage inflammatory activation) and VEGF-A and PDGF-BB (tissue repair and angiogenesis) were the only ones significantly increased in BAL from non-survivors compared to survivors (Figure 3A, CXCL4 mean pg/ml, 1487.8 [459.8-2798.7] vs 334.7 [111.9-630.6], p=0.048; VEGF-A mean pg/ml, 3481.8 [1308.7-6077.6] vs 335 [68.9-826.4], p=0.006; PDGF-BB mean pg/ml, 24 [6.7-43.5] vs 0, p=0.037; and S100A8 mean pg/ml, 5004.7 [1481.4-8762.9] vs 242.2 [63.53-484.4], p=0.01). This set of cytokines issued from or implicated with platelet/MK lineage which was enriched in non-survivor BAL pointed to a virus-mediated MK impairment and retention in the lung, as already observed in the bone marrow in deadly COVID-19.

MKs appear specifically recruited into or retain within the lung in COVID-19 autopsy cases (3) together with endothelial damages (42, 43). We therefore searched for MKs in BAL from patients with severe COVID-19 (Table 3). In line with the infection that we observed in bone marrow MKs, pulmonary MKs, identifiable through their large size and multilobed nucleus harboring cytoplasmic SARS-CoV-2 (+) RNA were detected in the BAL of COVID-19 patients irrespective of outcome, signing their viral infection (Figure 3B and Figure S7B). When quantified by flow cytometry, a trend, although statistically non-significant, towards increase frequency of MKs and platelets among BAL cells from non-survivors compared to survivors was observed (Figure 3C, Figure S7C). The frequencies of both infected spike$^+$ MKs and virus-containing spike$^+$ platelets in total MK and platelet populations were significantly increased by 4 and 29-fold in BAL from non-survivors versus survivors, respectively (Figure 3D, Figure S7C) (mean % spike$^+$ MKs and platelets in BAL from non-survivors versus survivors, 9.5 [7.1-12.3] vs 2.3 [0.8-4.7], p=0.016, and 2.9 [0.8-6.5] vs 0.1 [0.07-0.2], p=0.029, respectively).

The lack of statistically significant correlation between the frequency of spike$^+$ platelets among total platelets recovered in BAL measured by flow cytometry and the viral load measured per ml of BAL by RT-qPCR (Figure S7D), further indicates that detection of virus in platelets is not a result of virus endocytosis by the latter.

Upon pathological examination of lung autopsy cases, a high density of MKs, identified by their size and the caterpillar appearance of their large nuclei, surrounded by fibrin webs, was detected by histochemistry (Table 2, Figure 3E upper). Furthermore, capillary walls were highly damaged lacking the usual covering endothelial layer. MKs were not only found within the pulmonary vessels but also entering the alveoli (Figure 3E lower) (Figure 3E lower inset) and in the alveolar space as confirmed after specific vWF immunolabelling (Figure 3F and Figure S7E) in line with the unexpected presence of MKs in the BAL. When quantified in non-COVID-19 (n=6) and COVID-19 (n=3) lung autopsies as described (44, 45), the quantities of MKs increased by almost fourfold (from 5.78 $\pm$4.97 to 20.25$\pm$6.99 cells per section (5 cm^2 and 5-7 μm thickness) in non-COVDI-19 vs COVID-19 autopsies: p=0.0015), as well as their mean diameter (52.98$\pm$21.98 μm in non-COVDI-19 vs 79.68$\pm$19.45 μm in COVID-19 autopsies: p=0.05) and nucleus size (26.6$\pm$1.1 μm in non-COVDI-19 vs to 30.3$\pm$1.2 μm in COVID-19 autopsies, p=0.044, Figure S7F).

Furthermore, as observed in bone marrow and in BAL, lung tissue MKs were found actively infected harboring replicative viral (-) RNA (Figure 3G). 21.33±12.1 % (n=3) of lung MKs are positive for SARS-CoV-2 RNA, and infected lung MK are 2.5±0.8(n=3) times more frequently detected in alveoli than in blood vessels in lung tissues (Figure S7A). This suggests that platelets containing SARS-CoV-2 could also be produced in the lung of deadly COVID-19 patients.

Accordingly, a rough estimation of (-) SARS-CoV-2 positive platelet in tissue autopsies was obtained by measuring the Pearson's correlation coefficients (46) for colocalization of SARS-CoV-2 RNA with CD41 after excluding the signal from large CD41+ polylobed MKs and including CD41 signal from anucleated bodies only. As a result, correlation coefficients are significantly higher in both lung and bone marrow tissues from COVID-19 individuals (Pearson's coefficient: 0.739±0.252 and 0.747±0.632, respectively) as compared with

non-COVID-19 individuals (Pearson's coefficient for lung and bone marrow tissues: 0.160±0.093 and 0122±0.056, respectively) ($p<0.005$, n=3).

Platelets containing SARS-CoV-2 are captured by pulmonary macrophages

The rupture of the endothelium from the lung capillaries and the epithelium covering the alveolar surface observed here in COVID-19 lung autopsies and as we reported (56) might let platelets penetrate the alveolar tissue and space. In turn macrophages could capture these platelets by hemophagocytosis (47-49), establishing a route to lung macrophage infection mediated by SARS-CoV-2-containing platelets and inflammatory modulation (50). Indeed, hemophagocytosed platelets were detected in macrophages in the alveolar tissue and alveolar space of COVID-19 autopsies (Figure 4A, Table 2). Furthermore, in BAL from additional severe COVID-19 patients (Table 3) those from non-survivors contained also platelets containing SARS-CoV-2 RNA (+) (Figure 4B).

When quantified by flow cytometry, BAL from non-survivors had increased frequencies of platelet-macrophage conjugates than survivors (Figure 4C and Figure S7C), mean frequency of platelet-macrophage conjugates among total macrophage in BAL from non-survivors versus survivors was 4.6 [3.5-5.8] vs 2.4 [1.5-3.3], respectively, p=0.011). However, the frequency of macrophages (Figure S7G left) and spike$^+$ lung macrophages (Figure S7G right) conjugated or not with platelets did not differ in BAL from non-survivors and survivors.

SARS-CoV-2 contained in platelets of non-survivors is infectious

Whereas circulating SARS-CoV-2 free particles are not usually detected in infected patients (10), SARS-CoV-2 infected cells are found not only in the lung, but also at extrapulmonary sites in deadly COVID-19 (9). We thus hypothesized that in these patients, infection could be spread by platelets containing SARS-CoV-2 present in the circulation and at the pulmonary level.

We first investigated whether SARS-CoV-2 contained by platelets could be titrated on non-phagocytic Vero cells using the very sensitive FISH-flow assay we validated using different concentrations of SARS-CoV-2 (Figure S8).

To measure the titer of SARS-CoV-2 within platelets, we had first to force the virus to exit platelets from within, namely purging, by activating platelet with thrombin receptor activating peptide (TRAP) (51) inducing virus release in the medium without platelet aggregation (52). Platelets from COVID-19 non-survivors, with confirmed detection of SARS-CoV-2, were thus treated or not with TRAP, and centrifuged to collect platelet supernatants referred to as releasates that were then titrated on Vero cells (Figure S9A). In paired samples of 3 different non-survivors, the percentage of SARS-CoV-2 RNA$^+$/dsRNA$^+$ Vero cells infected with TRAP-treated compared to untreated platelet releasates was statistically significantly higher (p=0.042), the later falling below the limit of detection established using healthy donor platelet controls (Figure 4D and Figure S9B). Estimating Vero cell infection in PFU using the PFU/FISH-flow standard curve (Figure S8D), the mean

titer of SARS-CoV-2 virus sheltered in platelets and released by activating platelets was 35 [CI: 19-50] SARS-CoV-2 PFU per million platelets from COVID-19 non-survivors (n=3) (Figure 4D).

SARS-CoV-2 trans-infection from platelets to macrophages is blocked by anti-platelet drug abciximab

Platelets are short-lived and are mainly eliminated following their capture by tissue macrophages (53). Furthermore, lung macrophages express the main receptors for the virus necessary for infection (ACE2 and TMPRSS2) (54-56). Lung macrophages are found infected in COVID-19 and support SARS-CoV-2 replication *in vitro* as we and others have demonstrated recently (57-60), being a key cell in promoting viral spread (57-60), and the cytokine storm driving severe COVID-19 (50). Primary macrophages derived from blood monocytes (MDM) cultivated with M-CSF, interleukin (IL)-4 and IL-13 mimic tissue macrophages (22, 61) express ACE2 and TMPRSS2, support SARS-CoV-2 replication and self-limiting release of infectious viruses (Figure S10A-D). These MDM were cultivated with platelets from non-survivors for 2 hours (pulse), extensively washed and further cultivated for 24 hours (chase). Both viral (+) and (-) strands RNA indicative of virus replication were detected in macrophage cytosol after *in situ* hybridization and confocal microscopy analysis (Figure 4E). In contrast, after the pulse, only the (+) RNA signal corresponding to the platelet inoculum was detected in MDM (Figure 4E left). Viral RNA signal was also undetectable after incubation with platelets from survivors (not shown). Replication-competent virus was detected in the supernatant of the MDM-platelet co-culture 24 hours after inoculation with virus-containing platelets (Figure 4F left image and middle graph) using Vero cells as in (62). In contrast, no viral signal was detected after the pulse (Figure 4F middle, % of SARS-CoV-2 RNA^+/$dsRNA^+$ Vero cells infected by the supernatant of MDM incubated with platelets samples from non-survivor after the pulse vs the chase, 0 vs 1.07 % [0.6-1.5], p=0.029). When titrated on Vero reporter cells, plasma deprived of platelets (Platelet-poor plasma: PPP) from survivors and non-survivors were not infectious (Figure S10E left) revealing the absence of infectious virus in the circulation despite viral gene detection. In contrast, plasma containing SARS-CoV-2 -positive platelets added to macrophages resulted in the production of infectious viral particles, titrated on Vero reporter cells (Figure S10E right).

Finally, the SARS-CoV-2-containing platelet to MDM trans-infection process was blocked when platelets were pre-incubated with an anti-platelet GPIIbIIIa drug, abciximab, prior to MDM inoculation. In the presence of abciximab, the production of replication-competent virus by MDM after 24hrs infection was reduced by 98$\pm$0.9% (p<0.001) (Figure 4F right graph).

Discussion

Platelet activation, thrombophilia and hypercoagulability have emerged as crucial pathological characteristics in severe COVID-19 that can lead to fatal outcome (1). Hence, the frequency of thrombotic events in critical COVID-19 cases is particularly high, with increased frequency of venous and arterial thrombosis resulting in clinical complications including pulmonary embolism, ischemic stroke, and myocardial infarction (2, 6). Increased platelet activation has been shown as a poor prognostic factor (34). Previous studies have shown the presence of SARS-CoV-2 components in platelets in the context of COVID-19 platelet hyperactivation

(24) (25).

Here we not only demonstrate for the first time the presence of replication-competent functional virus in platelets but also correlate the detection of virus-containing platelets with patient outcome. In addition to contribution to life-threatening thrombotic disorders described in COVID (1, 2), we now show that platelets can also harbor infectious SARS-CoV-2 detected as early as three weeks prior to death (median [IQR] days from sampling to death: 7 [5;10] [from 1 to 20]) (Table 1). Furthermore, in patients with COVID-19, the presence of infectious SARS-CoV-2 in platelets is a strong predictive marker of fatal outcome. The detection of SARS-CoV-2 in platelets by RT-qPCR or FISH-Flow, easily implementable as a routine analysis, could serve as a diagnostic useful tool to foresee as early as possible poor prognosis and take appropriate medical action.

The present results prompt three questions: how does the virus enter platelets, what is the possible causal effect of the presence of virus in platelets in COVID-19 pathology, and which type of treatment might prevent these effects.

As we found MKs, the platelet precursors, actively infected in bone marrow and the lung in fatal forms of the disease, SARS-CoV-2 might likely associate with platelet during thrombopoiesis, in a process we and other demonstrated for HIV (22, 63), Dengue and Influenza virus (23) (21). Alternatively, platelets could endocytose the virus in the circulation as they express SARS-CoV-2 receptors such as ACE2 (64) and DC-SIGN that participate in virus endocytosis, as we have shown *in vitro* (18, 65, 66). It is however unlikely as free SARS-CoV-2 in platelet-poor plasma is not infectious and as platelets could not internalize SARS-CoV-2 *in vitro*.

Small MKs that reach the peripheral circulation after fragmentation from bone marrow and lung MKs (37, 38, 67), especially in inflammatory lung diseases (41), are present at low levels in PBMCs and can thus serve as surrogates in the analysis of human lung MKs, the access of which is challenging. Some of these circulating MKs harbor immunomodulatory functions in healthy donors (41, 68, 69). Similarly, we found in the blood from COVID-19 non-survivors a significant increase of circulating MKs carrying type I IFN and inflammatory gene signatures and an upregulation of genes conditioned by NFKB1, characteristics of a response to viral infection including that to SARS-CoV-2 (70). The expression of inflammatory genes typically involved in MK anti-viral response, such as IFITM1 and IFTIM3 (21), together with the non-classical MK differentiation pathway that we observed support the development of an emergency megakaryopoiesis in severe COVID-19 avoiding the MEP commitment (71). Such shortened pathway might be followed by an increase in MK number and size as we observed in bone marrow and lung tissues in COVID-19 compared to non-COVID-19 autopsies. Furthermore, we found in the lung of non-survivors an increase of CCL5, IL-1beta and IL6, cytokines inducing the production of thrombopoietin (TPO) that in turn speed megakaryopoiesis up, through the direct non-classical pathway (71). Additionally, such increased CCL5, known to stimulate MK ploidy (71) and in turn speed megakaryopoiesis, could explain the increase in MK nucleus size we found in COVID-19 compared with non-COVID-19 lung autopsies.

Altogether, in line with the emergency myelopoiesis that we reported earlier (72), these results point to a MK response to pathogenic stimuli, i.e., infection by SARS-CoV-2 of MKs in the bone marrow, before entry in the circulation. Infected MKs would then migrate from bone marrow to the lung and produce platelets containing SARS-CoV-2 at both sites as we specifically detected in non-survivors: this finding being likely connected to COVID-19 fatal immunothrombosis.

However, patient platelet counts monitored during the following 15 days or until discharge for the non-survivors (Figure S1A) did not show the appearance of thrombocytopenia or significant variation in platelets counts in both patient sets. Of note, the increase in megakaryocyte numbers observed in autopsy tissues from COVID versus non COVID patients is not accompanied by an increase in platelet numbers during deadly COVID. This observation suggests either an inefficient thrombopoiesis due to shortened megakaryopoiesis; or alternatively, a retention of megakaryocytes in the lung of patients with an inefficient platelet production and, as megakaryocytes are known to contain high amounts of growth factors and cytokines (73), they could in turn participate to a local cytokine storm.

MKs might also exert immunological functions by using the set of histone-associated genes that we found specifically increased in non-survivor inflammatory MKs. This may generate extra-nuclear histones that serve as damage-associated molecular patterns (DAMP) (74, 75), and participate in severing systemic inflammation and immunothrombosis in COVID-19 as it has been shown in sepsis (76, 77).

Infected MKs themselves would also participate to the cytokine storm by upregulation of interferon type I gene, as in other viral infections (21, 33, 78) and contribute to differential expression of virus-induced lung cytokines implicated in hemostasis and inflammation in COVID-19 non-survivors. Hence, PF4/CXCL4 is synthesized by MK and packaged within platelets alpha-granules during platelet production (13). Increase in PF4 in BAL from non-survivors might reflect both MK destruction in pulmonary vessels and platelet activation, shown to occur in COVID-19 patients (34). In turn, PF4 could intensify inflammation by polarizing lung tissue macrophages to the M4 inflammatory subtype (79) resulting in S100A8 secretion, thereby fueling inflammation (72, 79). VEGF-A and PDGF-BB, expressed in particular by myeloid cells including MKs and macrophages (80) could represent stress responses to pulmonary endothelium damage (81, 82) that we observed in pulmonary autopsy tissues. VEGF-A binds to Neuropilin 1 (NRP1) on endothelial cells contributing to the integrity of the vessel wall and to the inhibition of platelet aggregation in blood vessels (80, 83). SARS-CoV-2 spike protein that binds also to NRP1 (84, 85), may displace VEGF-A resulting in the increased levels of VEGF-A that we detected in COVID+ BAL and meanwhile facilitate small vessel thrombosis by inhibiting endothelial function both systemically and in the pulmonary circulation. In sum, the uncontrolled cytokine release may contribute to endothelial wall injuries (86) that would allow entrance of MKs and platelets to the alveolar space as assessed by bronchoalveolar lavage observation. This process appears specific to COVID-19, increased in non-survivors, although remaining limited in survivors.

Fully functional SARS-CoV-2 virus found within circulating platelets of non-survivors is infectious as in other viral infections (20, 22) indicating that SARS-CoV-2 viruses, protected by the platelet membrane from degradation by assault of antibodies or complement, might disseminate to other tissues. Virus would then propagate infection contributing to rapid multiple organ failure (87, 88). Accordingly, non-survivors in this

study reach a fatal issue within two weeks after symptom onset (Table 1) when virus is still replicating (10). We demonstrate that platelets harboring SARS-CoV-2 are capable to trans-infect macrophages *in vitro*, a process abrogated by the anti-platelet GPIIbIIIa drug abciximab. We have already shown that blocking platelet GPIIbIIIa with abciximab fully prevents platelets internalization by macrophages (22) although by a mechanism that is not yet demonstrated. We can hypothesize that platelet GPIIbIIIa interacts with either macrophage CD40 (89) or the integrin Mac1 ($\alpha M\beta 2$) in the presence of fibrinogen (90, 91) likely associated to platelets in our experimental conditions (Platelet Rich Plasma), promoting an outside-in GPIIbIIIa mechanism of activation that in turn promotes platelet uptake by macrophages (92) in a $\beta 2$-mediated phagocytosis process (93). Abciximab would impair such interactions and in turn, platelet induced macrophage infection and/or possibly activation. This hypothesis remains to be verified.

In COVID-19 patients lung tissue macrophages that we and other have found infected (57-60) may act as a Trojan horse, capable of transferring SARS-CoV-2 to nearby lung regions and in turn slowly propagating SARS-CoV-2 infection and spreading hyperinflammation across the lung (57-60) as witnessed by the increase in lung inflammatory cytokines we reported here. Upon phagocytosis by macrophages, SARS-CoV-2-containing platelets might transfer infection to macrophages that would produce IFN (94). Incoming viral RNA could also signal PRR to enhance phagocytosis, increase oxidative burst and release of pro-inflammatory cytokines and chemokines, resulting in inflammation. This would promote an influx of monocytes HLA-DR low S100A8+ into the lung, sustaining inflammation and tissue damage (60). Furthermore, platelet hyperactivation might be induced by virus or viral components within platelets resulting in exposure of vWF (this study) and P-Selectin (34) followed by platelet aggregation, which could contribute to lung inflammation as in influenza virus infection (95), and also been prevented by anti-GPIIbIIIa drug. Therefore, therapeutic targeting of the platelet surface protein GPIIbIIIa could help blocking the process of viral spread in addition to its anti-thrombotic effect.

The following features we observed in non-survivors, namely increased phagocytosis of virus-containing platelets, endothelial cell wall injury and the infection of MKs themselves, also occurring in other viral infection (21, 33, 78), may likely result in exacerbated macrophage-dependent cytokine production, increasing thrombotic risk and complications (86), a hallmark of severe COVID-19. These deleterious effects of platelets harboring SARS-CoV-2 are summarized and schematized altogether in Figure 5. Drugs targeting specifically the platelet receptor GPIIbIIIa may offer an alternative to scantily efficient anticoagulant treatment (6, 96): indeed, its direct and indirect anti-thrombotic effect, prevention of macrophage infection and activation limiting their contribution to the cytokine storm, in addition to impairing the spread of infection to other tissue represent a valuable therapeutic recourse. Accordingly, a clinical trial using an anti-GPIIbIIIa drug in critically ill patients with COVID-19 has shown a beneficial effect on respiratory functions and clinical outcome (97). In any case, the strategy of modifying platelet behavior needs careful consideration in the light of the results presented here. Indeed, it appears that platelets from severe COVID-19 patients bear a dual prothrombotic effect: via virally induced platelet activation and via decrease in endothelial function caused by the virus blocking the effect of VEGF-A at the NRP1 receptor which may be considered as an appropriate therapeutical target.

The present study may likely apply to patients infected with various SARS-CoV-2 variants. Our study was performed in France during the first wave of COVID-19 between April and June 2020 with samples from patients infected by the ancestral Wuhan virus SARS-CoV-2 before the appearance of the following variants (98). SARS-CoV-2 variants still use ACE2/TMPRSS2 for infection, although with different affinities (99). Thus, variants might likely infect megakaryocytes resulting in the production of platelets containing SARS-CoV-2 that would likewise trans-infect macrophages. We cannot rule out the possibility that infection by different variants would not affect megakaryocyte transcriptome (regulation) and in turn the genes transferred to platelets during thrombopoiesis and downstream effects.

The scarce availability of platelet samples and the relative low frequency of virus-containing platelets, hindering detection by traditional techniques such as plaque assay is a limitation of this study. Hence, we applied the more sensitive single-cell FISH-flow technique (22) to approach infectious SARS-CoV-2. Importantly, the estimated quantity of infectious virus sheltered by platelets is non-negligible, being of 35 [CI: 19-50] SARS-CoV-2 PFU per million platelets. Severe COVID-19 patients with fatal outcome appears to harbor 3.7-3.9 $\log_{10}$ platelet-associated SARS-CoV-2 PFU per ml of blood in the circulation. In addition, the contribution of the lung, the main site affected in severe COVID-19, has recently been estimated to half of the total platelet production with the lung producing 10 million platelets per hour (37). This would translate into a lung production of around 2 $\log_{10}$ platelet-associated SARS-CoV-2 PFU/hour.

In sum, the presence of infectious SARS-CoV-2 in platelet combined with the intricate relationship between hemostasis, inflammation and the spread of infection has major consequences on COVID-19 pathogenesis and can turn out fatal. Anti-platelet drugs might be explored to develop anti-inflammatory coupled to pro-thrombotic treatment against severe SARS-CoV-2.

Acknowledgments: The authors thank Professor John F. Martin (University College of London, UK) for fruitful advice and discussion on the role of NRP1 receptor and VEGF in COVID19 and resultant therapeutical implications, and for English editing. The authors greatly acknowledge Karine Bailly and Muriel Andrieu of the Cochin Cytometry and Immunobiology Facility for cytokine analyses, as well as Thomas Guilbert from the Imag'IC facility for instruction on the IXplore Spin Confocal Imaging Microscope System (Olympus) during the COVID-19 confinement period. We also thank also Dr. Nicolas Chapuis (Hopital Cochin, Paris, France) and Pr. Nicholas Heming (Raymond Poincaré Hospital, Garches, France) for helpful discussion.

Funding: Joint funding by the Agence Nationale de la Recherche (France) and Fondation pour la Recherche Médicale (France): Flash COVID ANR-FRM: ANR-20-COVI-0024. Funders of the study had no role in study design, data collection, data analysis, data interpretation, or writing of the manuscript. AZ was supported by the China Scholarship Council.

Declaration of Interests: The authors have no conflict of interest to declare.

Author Contributions: Study design: AZ, FR, CC, EE, ECB, and MB; Methodology: AZ, FR, CC, GLG, EE, SC, EE, and MB; Sample Resources: CC, AR, PM, SB, MG, GG, JDC, DA, and GLG ; Investigation: AZ, FR,

CC, JZ, JMM, SB, SV, EE, GLG, SC, ECB and MB; Formal data analysis, AZ, FR, EE, SC, ECB and MB ; Data interpretation: AZ, FR, EE, ECB and MB ; scRNAseq data analysis and interpretation: AS, FG, FR, GD and MB; Funding acquisition: MB ; Medical Validation: ECB, DA ; Writing – Original Draft, MB; Writing, review, editing, FR, ECB, and MB.

List of Supplementary Materials

References

1. Driggin E, Madhavan MV, Bikdeli B, Chuich T, Laracy J, Biondi-Zoccai G, et al. Cardiovascular Considerations for Patients, Health Care Workers, and Health Systems During the COVID-19 Pandemic. J Am Coll Cardiol. 2020;75(18):2352-71.
2. Klok FA, Kruip M, van der Meer NJM, Arbous MS, Gommers D, Kant KM, et al. Incidence of thrombotic complications in critically ill ICU patients with COVID-19. Thromb Res. 2020;191:145-7.
3. Rapkiewicz AV, Mai X, Carsons SE, Pittaluga S, Kleiner DE, Berger JS, et al. Megakaryocytes and platelet-fibrin thrombi characterize multi-organ thrombosis at autopsy in COVID-19: A case series. EClinicalMedicine. 2020;24:100434.
4. Bernardes JP, Mishra N, Tran F, Bahmer T, Best L, Blase JI, et al. Longitudinal Multi-omics Analyses Identify Responses of Megakaryocytes, Erythroid Cells, and Plasmablasts as Hallmarks of Severe COVID-19. Immunity. 2020;53(6):1296-314 e9.
5. Zhou X, Li Y, Yang Q. Antiplatelet Therapy After Percutaneous Coronary Intervention in Patients With COVID-19: Implications From Clinical Features to Pathologic Findings. Circulation. 2020;141(22):1736-8.
6. Bikdeli B, Madhavan MV, Jimenez D, Chuich T, Dreyfus I, Driggin E, et al. COVID-19 and Thrombotic or Thromboembolic Disease: Implications for Prevention, Antithrombotic Therapy, and Follow-Up: JACC State-of-the-Art Review. J Am Coll Cardiol. 2020;75(23):2950-73.
7. Chu H, Chan JF, Yuen TT, Shuai H, Yuan S, Wang Y, et al. Comparative tropism, replication kinetics, and cell damage profiling of SARS-CoV-2 and SARS-CoV with implications for clinical manifestations, transmissibility, and laboratory studies of COVID-19: an observational study. Lancet Microbe. 2020;1(1):e14-e23.

8. Hoffmann M, Kleine-Weber H, Schroeder S, Kruger N, Herrler T, Erichsen S, et al. SARS-CoV-2 Cell Entry Depends on ACE2 and TMPRSS2 and Is Blocked by a Clinically Proven Protease Inhibitor. Cell. 2020;181(2):271-80 e8.
9. Martines RB, Ritter JM, Matkovic E, Gary J, Bollweg BC, Bullock H, et al. Pathology and Pathogenesis of SARS-CoV-2 Associated with Fatal Coronavirus Disease, United States. Emerg Infect Dis. 2020;26(9):2005-15.
10. Wolfel R, Corman VM, Guggemos W, Seilmaier M, Zange S, Muller MA, et al. Virological assessment of hospitalized patients with COVID-2019. Nature. 2020;581(7809):465-9.
11. Trypsteen W, Van Cleemput J, Snippenberg WV, Gerlo S, Vandekerckhove L. On the whereabouts of SARS-CoV-2 in the human body: A systematic review. PLoS Pathog. 2020;16(10):e1009037.
12. Moustafa A, Khalel RS, Aziz RK. Traces of SARS-CoV-2 RNA in Peripheral Blood Cells of Patients with COVID-19. OMICS. 2021;25(8):475-83.
13. Semple JW, Italiano JE, Jr., Freedman J. Platelets and the immune continuum. Nat Rev Immunol. 2011;11(4):264-74.
14. Boilard E, Pare G, Rousseau M, Cloutier N, Dubuc I, Levesque T, et al. Influenza virus H1N1 activates platelets through FcgammaRIIA signaling and thrombin generation. Blood. 2014;123(18):2854-63.
15. Rondina MT, Brewster B, Grissom CK, Zimmerman GA, Kastendieck DH, Harris ES, et al. In vivo platelet activation in critically ill patients with primary 2009 influenza A(H1N1). Chest. 2012;141(6):1490-5.
16. Kapur R, Zufferey A, Boilard E, Semple JW. Nouvelle cuisine: platelets served with inflammation. J Immunol. 2015;194(12):5579-87.
17. Morrell CN, Aggrey AA, Chapman LM, Modjeski KL. Emerging roles for platelets as immune and inflammatory cells. Blood. 2014;123(18):2759-67.
18. Assinger A. Platelets and infection - an emerging role of platelets in viral infection. Front Immunol. 2014;5:649.
19. Garraud O, Cognasse F. Are Platelets Cells? And if Yes, are They Immune Cells? Front Immunol. 2015;6:70.
20. Simon AY, Sutherland MR, Pryzdial EL. Dengue virus binding and replication by platelets. Blood. 2015;126(3):378-85.
21. Campbell RA, Schwertz H, Hottz ED, Rowley JW, Manne BK, Washington AV, et al. Human megakaryocytes possess intrinsic antiviral immunity through regulated induction of IFITM3. Blood. 2019;133(19):2013-26.
22. Real F, Capron C, Sennepin A, Arrigucci R, Zhu A, Sannier G, et al. Platelets from HIV-infected individuals on antiretroviral drug therapy with poor CD4(+) T cell recovery can harbor replication-competent HIV despite viral suppression. Sci Transl Med. 2020;12(535).
23. Vogt MB, Lahon A, Arya RP, Spencer Clinton JL, Rico-Hesse R. Dengue viruses infect human megakaryocytes, with probable clinical consequences. PLoS Negl Trop Dis. 2019;13(11):e0007837.
24. Manne BK, Denorme F, Middleton EA, Portier I, Rowley JW, Stubben C, et al. Platelet gene expression and function in patients with COVID-19. Blood. 2020;136(11):1317-29.
25. Zaid Y, Puhm F, Allaeys I, Naya A, Oudghiri M, Khalki L, et al. Platelets Can Associate with SARS-Cov-2 RNA and Are Hyperactivated in COVID-19. Circ Res. 2020.
26. Laue M, Kauter A, Hoffmann T, Michel J, Nitsche A. Morphometry of SARS-CoV and SARS-CoV-2 particles in ultrathin sections of infected Vero cell cultures. bioRxiv. 2020:2020.08.20.259531.
27. Hosier H, Farhadian SF, Morotti RA, Deshmukh U, Lu-Culligan A, Campbell KH, et al. SARS–CoV-2 infection of the placenta. The Journal of Clinical Investigation. 2020;130(9):4947-53.
28. Mohanty SK, Satapathy A, Naidu MM, Mukhopadhyay S, Sharma S, Barton LM, et al. Severe acute respiratory syndrome coronavirus-2 (SARS-CoV-2) and coronavirus disease 19 (COVID-19) – anatomic pathology perspective on current knowledge. Diagnostic Pathology. 2020;15(1):103.
29. Bullock HA, Goldsmith CS, Zaki SR, Martines RB, Miller SE. Difficulties in Differentiating Coronaviruses from Subcellular Structures in Human Tissues by Electron Microscopy. Emerg Infect Dis. 2021;27(4):1023-31.
30. Martin-Cardona A, Lloreta Trull J, Albero-Gonzalez R, Paraira Beser M, Andujar X, Ruiz-Ramirez P, et al. SARS-CoV-2 identified by transmission electron microscopy in lymphoproliferative and ischaemic intestinal lesions of COVID-19 patients with acute abdominal pain: two case reports. BMC Gastroenterol. 2021;21(1):334.
31. van Nispen tot Pannerden H, de Haas F, Geerts W, Posthuma G, van Dijk S, Heijnen HF. The platelet interior revisited: electron tomography reveals tubular alpha-granule subtypes. Blood. 2010;116(7):1147-56.
32. Noisakran S, Gibbons RV, Songprakhon P, Jairungsri A, Ajariyakhajorn C, Nisalak A, et al. Detection of dengue virus in platelets isolated from dengue patients. Southeast Asian J Trop Med Public Health. 2009;40(2):253-62.
33. Jansen AJG, Spaan T, Low HZ, Di Iorio D, van den Brand J, Tieke M, et al. Influenza-induced thrombocytopenia is dependent on the subtype and sialoglycan receptor and increases with virus pathogenicity. Blood Adv. 2020;4(13):2967-78.

34. Hottz ED, Azevedo-Quintanilha IG, Palhinha L, Teixeira L, Barreto EA, Pao CRR, et al. Platelet activation and platelet-monocyte aggregate formation trigger tissue factor expression in patients with severe COVID-19. Blood. 2020;136(11):1330-41.
35. Moustafa A, Aziz RK. Traces of SARS-CoV-2 RNA in the Blood of COVID-19 Patients. medRxiv. 2020:2020.05.10.20097055.
36. Levine RF, Eldor A, Shoff PK, Kirwin S, Tenza D, Cramer EM. Circulating megakaryocytes: delivery of large numbers of intact, mature megakaryocytes to the lungs. Eur J Haematol. 1993;51(4):233-46.
37. Lefrancais E, Ortiz-Munoz G, Caudrillier A, Mallavia B, Liu F, Sayah DM, et al. The lung is a site of platelet biogenesis and a reservoir for haematopoietic progenitors. Nature. 2017;544(7648):105-9.
38. Ouzegdouh Y, Capron C, Bauer T, Puymirat E, Diehl JL, Martin JF, et al. The physical and cellular conditions of the human pulmonary circulation enable thrombopoiesis. Exp Hematol. 2018;63:22-7 e3.
39. Ren X, Wen W, Fan X, Hou W, Su B, Cai P, et al. COVID-19 immune features revealed by a large-scale single-cell transcriptome atlas. Cell. 2021;184(7):1895-913 e19.
40. Choudry FA, Bagger FO, Macaulay IC, Farrow S, Burden F, Kempster C, et al. Transcriptional characterization of human megakaryocyte polyploidization and lineage commitment. J Thromb Haemost. 2021;19(5):1236-49.
41. Couldwell G, Machlus KR. Modulation of megakaryopoiesis and platelet production during inflammation. Thromb Res. 2019;179:114-20.
42. Fox SE, Akmatbekov A, Harbert JL, Li G, Quincy Brown J, Vander Heide RS. Pulmonary and cardiac pathology in African American patients with COVID-19: an autopsy series from New Orleans. The Lancet Respiratory Medicine. 2020;8(7):681-6.
43. Roncati L, Ligabue G, Nasillo V, Lusenti B, Gennari W, Fabbiani L, et al. A proof of evidence supporting abnormal immunothrombosis in severe COVID-19: naked megakaryocyte nuclei increase in the bone marrow and lungs of critically ill patients. Platelets. 2020;31(8):1085-9.
44. Mason RJ. Pathogenesis of COVID-19 from a cell biology perspective. Eur Respir J. 2020;55(4).
45. Hu B, Tang Y, Chang EI, Fan Y, Lai M, Xu Y. Unsupervised Learning for Cell-Level Visual Representation in Histopathology Images With Generative Adversarial Networks. IEEE J Biomed Health Inform. 2019;23(3):1316-28.
46. Luu R, Valdebenito S, Scemes E, Cibelli A, Spray DC, Rovegno M, et al. Pannexin-1 channel opening is critical for COVID-19 pathogenesis. iScience. 2021;24(12):103478.
47. Wang C, Xie J, Zhao L, Fei X, Zhang H, Tan Y, et al. Alveolar macrophage dysfunction and cytokine storm in the pathogenesis of two severe COVID-19 patients. EBioMedicine. 2020;57:102833.
48. Labro G, Jandeaux LM, Rusu A, Virot E, Pointurier V, Pinto L, et al. Macrophage Activation in COVID-19 Patients in Intensive Care Unit2020.
49. Debliquis A, Harzallah I, Mootien JY, Poidevin A, Labro G, Mejri A, et al. Haemophagocytosis in bone marrow aspirates in patients with COVID-19. Br J Haematol. 2020;190(2):e70-e3.
50. Liao M, Liu Y, Yuan J, Wen Y, Xu G, Zhao J, et al. Single-cell landscape of bronchoalveolar immune cells in patients with COVID-19. Nat Med. 2020;26(6):842-4.
51. Piersma SR, Broxterman HJ, Kapci M, de Haas RR, Hoekman K, Verheul HM, et al. Proteomics of the TRAP-induced platelet releasate. J Proteomics. 2009;72(1):91-109.
52. Maguire PB, Parsons ME, Szklanna PB, Zdanyte M, Munzer P, Chatterjee M, et al. Comparative Platelet Releasate Proteomic Profiling of Acute Coronary Syndrome versus Stable Coronary Artery Disease. Front Cardiovasc Med. 2020;7:101.
53. Italiano JE, Jr. and Hartwig, J. Production and Destruction of Platelets. 2015.
54. Lukassen S, Chua RL, Trefzer T, Kahn NC, Schneider MA, Muley T, et al. SARS-CoV-2 receptor ACE2 and TMPRSS2 are primarily expressed in bronchial transient secretory cells. EMBO J. 2020;39(10):e105114.
55. Bertram S, Heurich A, Lavender H, Gierer S, Danisch S, Perin P, et al. Influenza and SARS-coronavirus activating proteases TMPRSS2 and HAT are expressed at multiple sites in human respiratory and gastrointestinal tracts. PLoS One. 2012;7(4):e35876.
56. Song X, Hu W, Yu H, Zhao L, Zhao Y, Zhao X, et al. Little to no expression of angiotensin-converting enzyme-2 on most human peripheral blood immune cells but highly expressed on tissue macrophages. Cytometry A. 2020.
57. Valdebenito S, Bessis S, Annane D, Lorin de la Grandmaison G, Cramer-Borde E, Prideaux B, et al. COVID-19 Lung Pathogenesis in SARS-CoV-2 Autopsy Cases. Front Immunol. 2021;12:735922.
58. Sefik E, Qu R, Kaffe E, Zhao J, Junqueira C, Mirza H, et al. Viral replication in human macrophages enhances an inflammatory cascade and interferon driven chronic COVID-19 in humanized mice. bioRxiv. 2021.
59. Grant RA, Morales-Nebreda L, Markov NS, Swaminathan S, Querrey M, Guzman ER, et al. Circuits between infected macrophages and T cells in SARS-CoV-2 pneumonia. Nature. 2021;590(7847):635-41.
60. Knoll R, Schultze JL, Schulte-Schrepping J. Monocytes and Macrophages in COVID-19. Front Immunol. 2021;12:720109.

61. Ganor Y, Real F, Sennepin A, Dutertre CA, Prevedel L, Xu L, et al. HIV-1 reservoirs in urethral macrophages of patients under suppressive antiretroviral therapy. Nat Microbiol. 2019;4(4):633-44.
62. Ogando NS, Dalebout TJ, Zevenhoven-Dobbe JC, Limpens R, van der Meer Y, Caly L, et al. SARS-coronavirus-2 replication in Vero E6 cells: replication kinetics, rapid adaptation and cytopathology. J Gen Virol. 2020;101(9):925-40.
63. Zucker-Franklin D, Cao YZ. Megakaryocytes of human immunodeficiency virus-infected individuals express viral RNA. Proc Natl Acad Sci U S A. 1989;86(14):5595-9.
64. Zhang S, Liu Y, Wang X, Yang L, Li H, Wang Y, et al. SARS-CoV-2 binds platelet ACE2 to enhance thrombosis in COVID-19. J Hematol Oncol. 2020;13(1):120.
65. Boukour S, Masse JM, Benit L, Dubart-Kupperschmitt A, Cramer EM. Lentivirus degradation and DC-SIGN expression by human platelets and megakaryocytes. J Thromb Haemost. 2006;4(2):426-35.
66. Flaujac C, Boukour S, Cramer-Borde E. Platelets and viruses: an ambivalent relationship. Cell Mol Life Sci. 2010;67(4):545-56.
67. Martin JF, Slater DN, Trowbridge EA. Abnormal intrapulmonary platelet production: a possible cause of vascular and lung disease. Lancet. 1983;1(8328):793-6.
68. Pariser DN, Hilt ZT, Ture SK, Blick-Nitko SK, Looney MR, Cleary SJ, et al. Lung megakaryocytes are immune modulatory cells. J Clin Invest. 2021;131(1).
69. Wang H, He J, Xu C, Chen X, Yang H, Shi S, et al. Decoding Human Megakaryocyte Development. Cell Stem Cell. 2021;28(3):535-49 e8.
70. Zheng M, Karki R, Williams EP, Yang D, Fitzpatrick E, Vogel P, et al. TLR2 senses the SARS-CoV-2 envelope protein to produce inflammatory cytokines. Nat Immunol. 2021.
71. Noetzli LJ, French SL, Machlus KR. New Insights Into the Differentiation of Megakaryocytes From Hematopoietic Progenitors. Arterioscler Thromb Vasc Biol. 2019;39(7):1288-300.
72. Silvin A, Chapuis N, Dunsmore G, Goubet AG, Dubuisson A, Derosa L, et al. Elevated Calprotectin and Abnormal Myeloid Cell Subsets Discriminate Severe from Mild COVID-19. Cell. 2020;182(6):1401-18 e18.
73. Cunin P, Nigrovic PA. Megakaryocytes as immune cells. J Leukoc Biol. 2019;105(6):1111-21.
74. Parseghian MH, Luhrs KA. Beyond the walls of the nucleus: the role of histones in cellular signaling and innate immunity. Biochem Cell Biol. 2006;84(4):589-604.
75. Xu Z, Huang Y, Mao P, Zhang J, Li Y. Sepsis and ARDS: The Dark Side of Histones. Mediators Inflamm. 2015;2015:205054.
76. Ekaney ML, Otto GP, Sossdorf M, Sponholz C, Boehringer M, Loesche W, et al. Impact of plasma histones in human sepsis and their contribution to cellular injury and inflammation. Crit Care. 2014;18(5):543.
77. Frydman GH, Tessier SN, Wong KHK, Vanderburg CR, Fox JG, Toner M, et al. Megakaryocytes contain extranuclear histones and may be a source of platelet-associated histones during sepsis. Sci Rep. 2020;10(1):4621.
78. Koupenova M, Corkrey HA, Vitseva O, Manni G, Pang CJ, Clancy L, et al. The role of platelets in mediating a response to human influenza infection. Nat Commun. 2019;10(1):1780.
79. Gleissner CA, Shaked I, Little KM, Ley K. CXC chemokine ligand 4 induces a unique transcriptome in monocyte-derived macrophages. J Immunol. 2010;184(9):4810-8.
80. Apte RS, Chen DS, Ferrara N. VEGF in Signaling and Disease: Beyond Discovery and Development. Cell. 2019;176(6):1248-64.
81. Teuwen LA, Geldhof V, Pasut A, Carmeliet P. COVID-19: the vasculature unleashed. Nat Rev Immunol. 2020;20(7):389-91.
82. O'Sullivan JM, Gonagle DM, Ward SE, Preston RJS, O'Donnell JS. Endothelial cells orchestrate COVID-19 coagulopathy. Lancet Haematol. 2020;7(8):e553-e5.
83. Nachman RL, Rafii S. Platelets, petechiae, and preservation of the vascular wall. N Engl J Med. 2008;359(12):1261-70.
84. Daly JL, Simonetti B, Antón-Plágaro C, Kavanagh Williamson M, Shoemark DK, Simón-Gracia L, et al. Neuropilin-1 is a host factor for SARS-CoV-2 infection. bioRxiv. 2020:2020.06.05.134114.
85. Cantuti-Castelvetri L, Ojha R, Pedro LD, Djannatian M, Franz J, Kuivanen S, et al. Neuropilin-1 facilitates SARS-CoV-2 cell entry and provides a possible pathway into the central nervous system. bioRxiv. 2020:2020.06.07.137802.
86. Buszko M, Park JH, Verthelyi D, Sen R, Young HA, Rosenberg AS. The dynamic changes in cytokine responses in COVID-19: a snapshot of the current state of knowledge. Nat Immunol. 2020;21(10):1146-51.
87. Zaim S, Chong JH, Sankaranarayanan V, Harky A. COVID-19 and Multiorgan Response. Curr Probl Cardiol. 2020;45(8):100618.
88. Wang T, Du Z, Zhu F, Cao Z, An Y, Gao Y, et al. Comorbidities and multi-organ injuries in the treatment of COVID-19. Lancet. 2020;395(10228):e52.
89. Prasad KS, Andre P, He M, Bao M, Manganello J, Phillips DR. Soluble CD40 ligand induces beta3 integrin tyrosine phosphorylation and triggers platelet activation by outside-in signaling. Proc Natl Acad Sci U S A. 2003;100(21):12367-71.

90. Bennett JS. Structure and function of the platelet integrin alphaIIbbeta3. J Clin Invest. 2005;115(12):3363-9.
91. Pretorius E. Platelets in HIV: A Guardian of Host Defence or Transient Reservoir of the Virus? Front Immunol. 2021;12:649465.
92. Ma YQ, Qin J, Plow EF. Platelet integrin alpha(IIb)beta(3): activation mechanisms. J Thromb Haemost. 2007;5(7):1345-52.
93. Sun H, Zhi K, Hu L, Fan Z. The Activation and Regulation of beta2 Integrins in Phagocytes and Phagocytosis. Front Immunol. 2021;12:633639.
94. Boumaza A, Gay L, Mezouar S, Bestion E, Diallo AB, Michel M, et al. Monocytes and Macrophages, Targets of Severe Acute Respiratory Syndrome Coronavirus 2: The Clue for Coronavirus Disease 2019 Immunoparalysis. J Infect Dis. 2021;224(3):395-406.
95. Le VB, Schneider JG, Boergeling Y, Berri F, Ducatez M, Guerin JL, et al. Platelet activation and aggregation promote lung inflammation and influenza virus pathogenesis. Am J Respir Crit Care Med. 2015;191(7):804-19.
96. Vivas D, Roldan V, Esteve-Pastor MA, Roldan I, Tello-Montoliu A, Ruiz-Nodar JM, et al. Recommendations on antithrombotic treatment during the COVID-19 pandemic. Position statement of the Working Group on Cardiovascular Thrombosis of the Spanish Society of Cardiology. Rev Esp Cardiol (Engl Ed). 2020;73(9):749-57.
97. Viecca M, Radovanovic D, Forleo GB, Santus P. Enhanced platelet inhibition treatment improves hypoxemia in patients with severe Covid-19 and hypercoagulability. A case control, proof of concept study. Pharmacol Res. 2020;158:104950.
98. Santé Publique France https://www.santepubliquefrance.fr/dossiers/coronavirus-covid-19/coronavirus-circulation-des-variants-du-sars-cov-2.
99. Hirabara SM, Serdan TDA, Gorjao R, Masi LN, Pithon-Curi TC, Covas DT, et al. SARS-COV-2 Variants: Differences and Potential of Immune Evasion. Front Cell Infect Microbiol. 2021;11:781429.

Figures and Figure legends

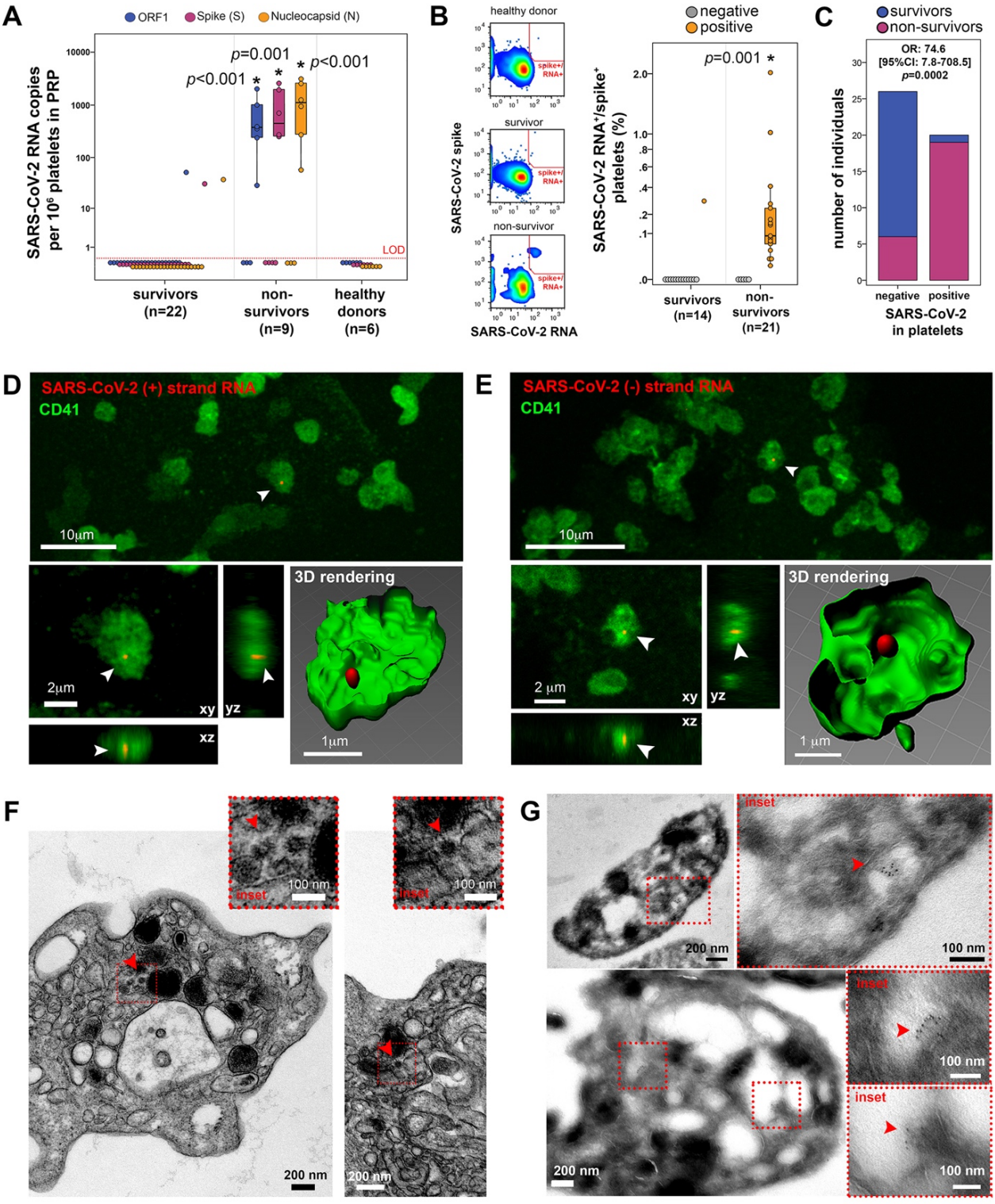

Figure 1: Platelets from non-survivor patients with COVID-19 harbor SARS-CoV-2.

A) Copies of SARS-CoV-2 ORF1 (blue), Spike (S, magenta) and Nucleocapsid (N, orange) RNA per million platelets detected by RT-qPCR, from COVID-19 survivors, COVID-19 non-survivors and healthy donor samples. Asterisk indicates statistical significance in the comparison between survivors and non-survivors per detected gene target (Kruskal-Wallis between the three groups). LOD=limit of detection.

B) Combined detection of SARS-CoV-2 spike protein and SARS-CoV-2 RNA by flow cytometry (FISH-flow). On the left, SARS-CoV-2 spike$^+$/RNA$^+$ detection gate (red) showing an example of healthy donor, COVID-19

survivor, and COVID-19 non-survivor. On the right, the percentage of SARS-CoV-2 spike$^+$/RNA$^+$ platelets among platelets from COVID-19 survivors and non-survivors, normalized by detected events in healthy donor samples. Samples were classified as negative (gray) or positive (orange) for the presence of SARS-CoV-2 in platelets. Asterisk indicates statistical significance in the comparison between survivors and non-survivors (Mann-Whitney between the two groups).

C) Number of COVID-19 survivors (blue) and non-survivors (magenta) among individuals tested for the presence of SARS-CoV-2 in platelets (negative or positive). OR: odds ratio.

D-E) Confocal microscopy images after CD41 (green) immunolabelling and SARS-CoV-2 RNA *in situ* hybridization (red) for SARS-CoV-2 (+) RNA (D) or SARS-CoV-2 (-) RNA (E) in platelet samples from a COVID-19 non-survivor. Images show low magnification (upper, bar=10μm), three-dimensional projections (lower left - xy, xz and yz, bar=2μm) and three-dimensional rendering (lower right, bar=1μm). Arrowheads indicate SARS-CoV-2 RNA, showing definite intracellular localization of the virus within the platelets.

F) Representative electron microscopy images of platelets with spherical crowned SARS-CoV-2 particles of 50-80nm in diameter (arrowheads) located in the lumen of OCS in platelets of non-survivors (bars= 200 nm). Dotted line indicates area magnified as shown in the insets (bar= 100 nm).

G) Immunogold labeling with a polyclonal anti-spike antibody of spike protein of non-survivor platelets otherwise tested positive for the presence of SARS-CoV-2 by FISH-Flow techniques (two examples, upper and lower images). Dotted squares point magnified regions where spike proteins were immunolocalized (red arrowhead). No spike immunolabeling was observed on platelet surface. Bar=100, 200 or 500 nm.

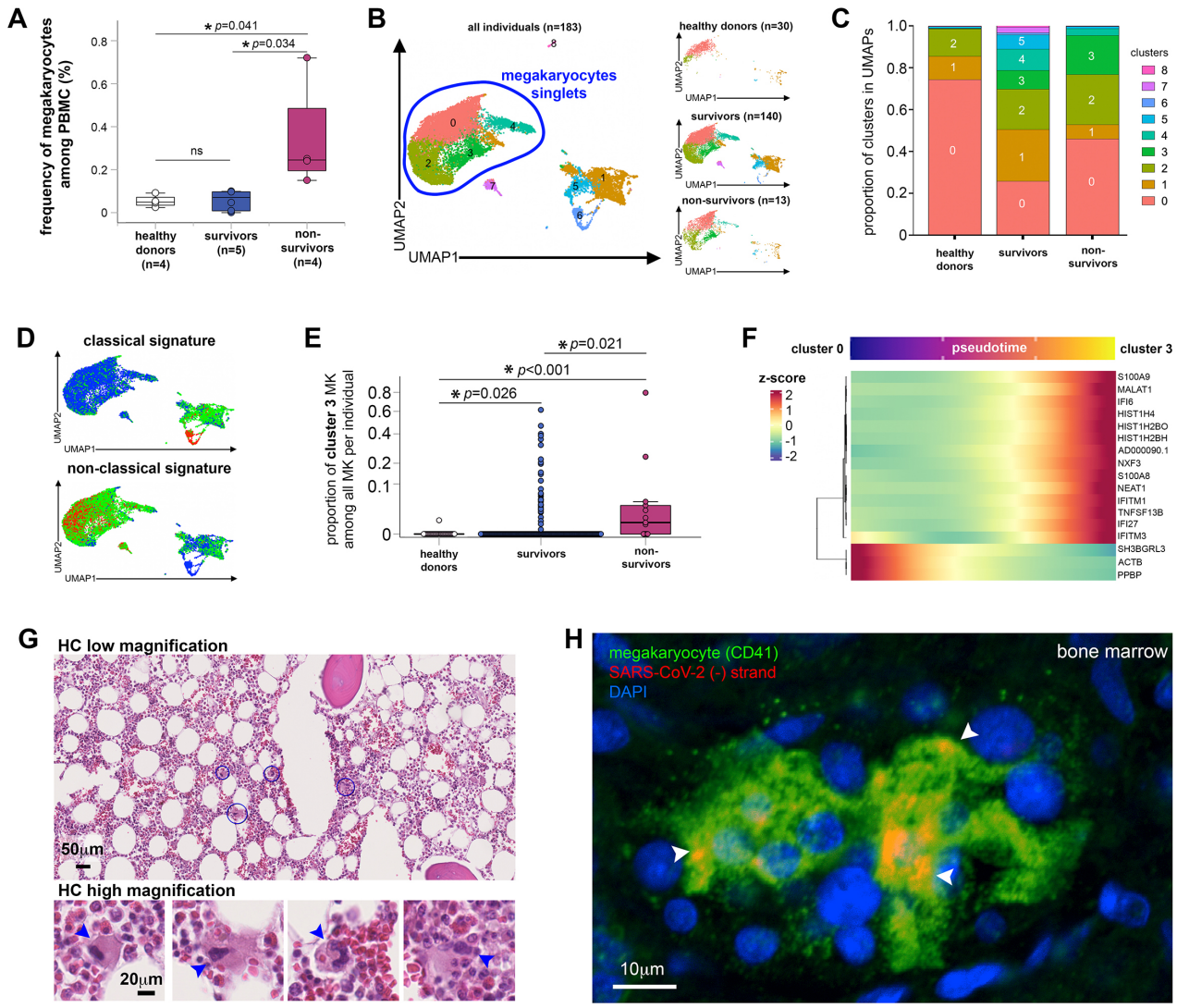

Figure 2: In COVID-19 non-survivors, MKs are infected and express viral sensing genes.

A) Frequency of MKs detected among PBMC from healthy donors and COVID-19 survivors and non-survivors as assessed by flow cytometry. Asterisks indicate statistical significance (Kruskal-Wallis test).

B-F) Transcriptional identity of MKs in COVID-19 patients by single-cell RNA sequencing reveals distinct phenotypes in non-survivor patients. B) UMAP of single-cell transcriptomic data of MKs detected among PBMC from non-COVID-19 healthy donors (n=30), COVID-19 survivors (n=140) and COVID-19 non-survivors (n=13). Unsupervised clustering detected 9 different clusters (0 to 8) of all cells analyzed. MK singlets are indicated by blue region. C) Proportion of each cluster in healthy donors, COVID-19 survivors and non-survivors. D) Scored gene signature expression of classical (upper) and non-classical (bottom) MK differentiation. E) Fraction of cells from cluster 3 in comparison to all other clusters in individual patient samples categorized as healthy donors, COVID-19 survivors and non-survivors. F) Heatmap of the genes that significantly change along pseudotime trajectory of MK development (p < 0.05 and Morans I score > 0.25).

G) Hematoxylin/eosin histology of bone marrow tissue obtained after COVID-19 non-survivor autopsy (low magnification (bar=50μm)) in which some MKs surrounded by blue circles are shown in high magnification insets (bar=20μm). Arrowheads indicate MKs.

H) Confocal microscopy images after CD41 (green) immunolabelling and replicative SARS-CoV-2 (-) RNA strand *in situ* hybridization (red) in bone marrow samples obtained from COVID-19 non-survivors autopsies (bar=10μm). Arrowheads indicate SARS-CoV-2 (-) RNA inside.

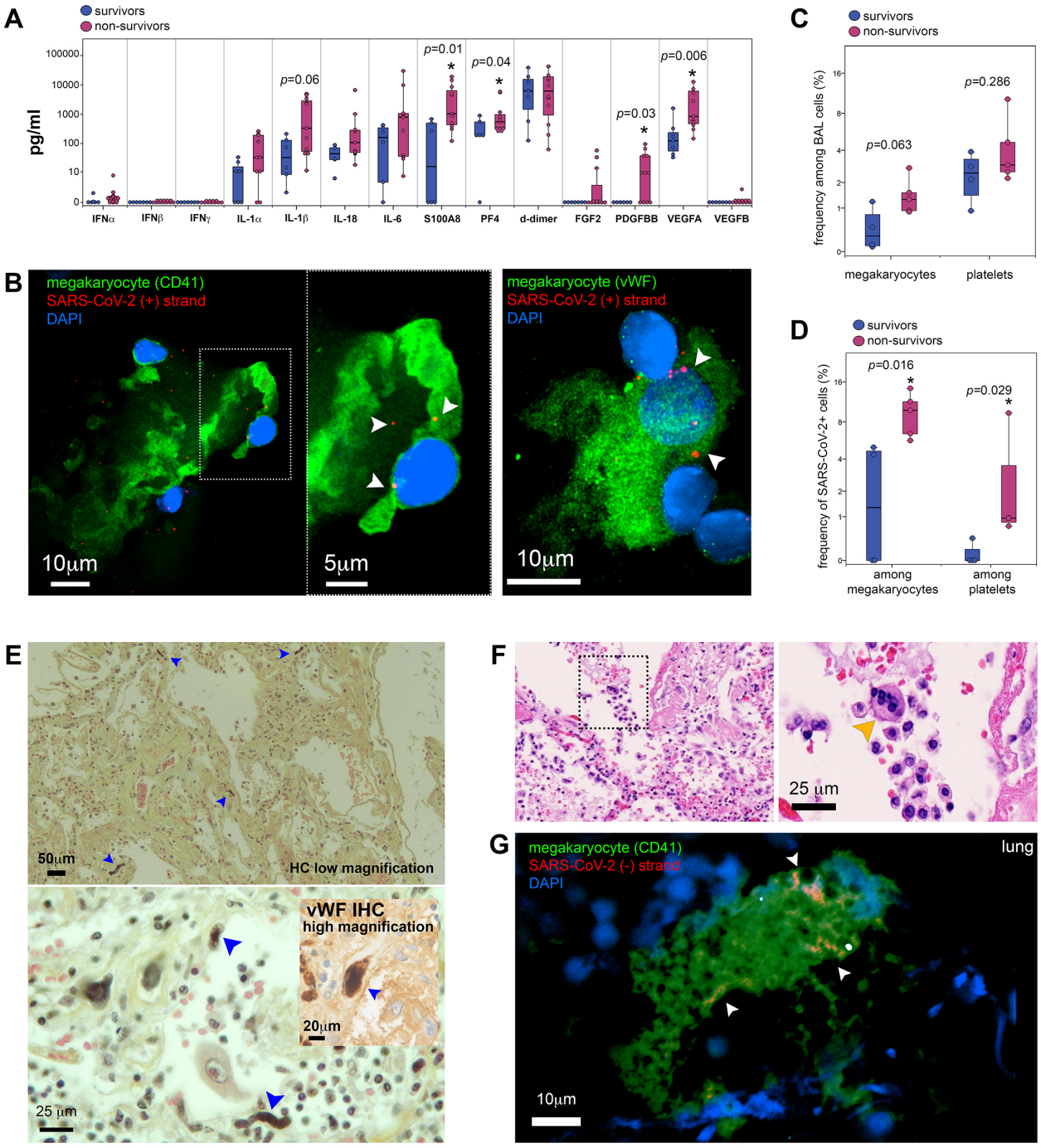

Figure 3: SARS-CoV-2 in platelets and MKs in lung from non-survivor COVID-19 patients.

A) Quantification of different cytokines/chemokines in bronchoalveolar lavage samples from COVID-19 survivors (blue) and non-survivors (magenta). Asterisk indicates statistical significance in the comparison between survivors and non-survivors (Mann-Whitney).

B) Confocal microscopy images after SARS-CoV-2 RNA *in situ* hybridization (red) for positive (+) RNA strand and immunolabelling of either CD41 (upper row) or vWF (lower row), both in green, in bronchoalveolar lavage samples from two different COVID-19 non-survivors (bar=10μm or 5μm for the inset in upper image). Arrowheads indicate SARS-CoV-2 RNA inside MKs.

C) Frequency of MKs and platelets among the cell population detected in bronchoalveolar lavage samples from COVID-19 survivors (blue) and non-survivors (magenta) detected by flow cytometry.

D) Frequency of SARS-CoV-2^{+} MKs and platelets among the population of MKs and platelets detected in bronchoalveolar lavage samples from COVID-19 survivors (blue) and non-survivors (magenta) as detected

by flow cytometry. Asterisk indicates statistical significance in the comparison between survivors and non-survivors (Mann-Whitney).

E) Hematoxylin/eosin/saffron histology and vWF immunohistochemistry (lower inset) of lung tissue from COVID-19 autopsy, showing low (bar=50μm) and high magnification (bar=20 and 25 μm) images. Blue arrowheads indicate MKs.

F) Hematoxylin/eosin histology of lung tissue in which some MKs indicated by dotted square region (left column), resided to reside inside alveolar space (right column) (bar=25 μm). Orange arrowheads indicate MKs.

G) Confocal microscopy images after CD41 (green) immunolabelling and replicative SARS-CoV-2 (-) RNA strand *in situ* hybridization (red) in lung samples obtained from COVID-19 non-survivors autopsies (bar=10μm). Arrowheads indicate SARS-CoV-2 (-) RNA inside MKs.

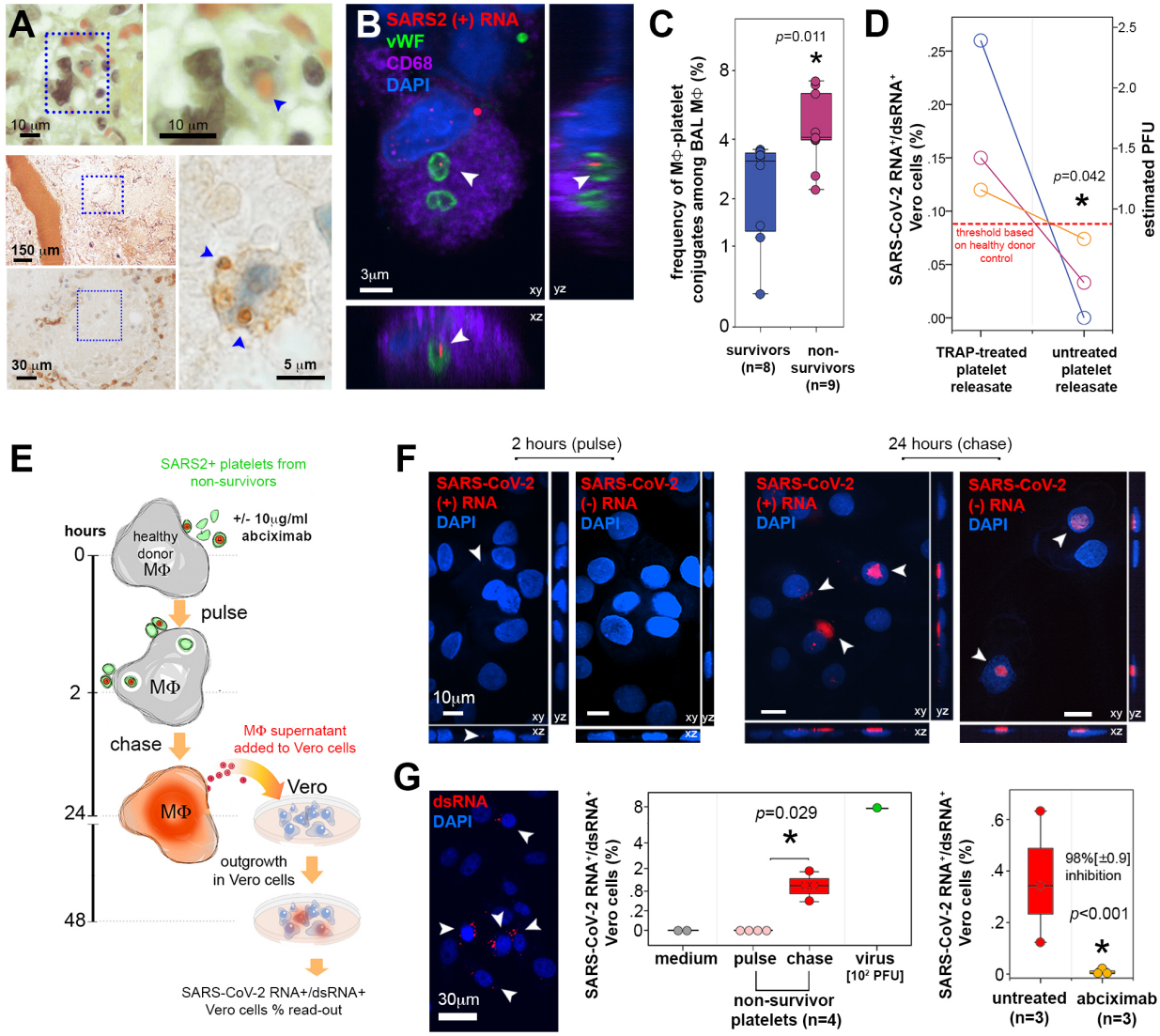

Figure 4: SARS-CoV-2 sheltered by platelets from non-survivor patients with COVID-19 is infectious to macrophages.

A) Upper row: Hematoxylin/eosin/saffron stain histology of lung tissue from a COVID-19 autopsy showing a macrophage, indicated by dotted square region (left) and shown in higher magnification (right) phagocytosing a red blood cell (blue arrowhead). Bar=10µm. Lower panel: Immunohistochemistry for vWF of alveoli from non-survivor lung autopsy (indicated by blue dotted square at low magnification, bar=150µm) where a macrophage (indicated by blue dotted square at middle magnification, bar=30µm) contained hemophagocytosed vWF$^+$ platelets (blue arrowheads in high magnification image, bar=5µm).

B) Representative confocal microscopy images after vWF (green) and CD68 (purple) immunolabelling and SARS-CoV-2 RNA *in situ* hybridization (red) for positive (+) RNA strand in bronchoalveolar lavage samples from COVID-19 non-survivors. Images show three-dimensional projections (xy, xz and yz, bar=3µm). Arrowheads indicate SARS-CoV-2 RNA inside platelets engulfed by macrophages (representative of n=3 different individuals).

C) Frequency of macrophage-platelet conjugates among macrophages in bronchoalveolar lavage samples from COVID-19 survivors (blue) and non-survivors (magenta) detected by flow cytometry. Asterisk indicates statistical significance in the comparison between survivors and non-survivors (Mann-Whitney).

D) Paired comparison of percentages of SARS-CoV-2 RNA^+/$dsRNA^+$ Vero cells treated with releasate from platelets treated or not with TRAP, from 3 different non-survivors. The detection threshold (dotted red line) was established with healthy donor platelets treated equally. The percentages were converted in PFU per million platelets using the standard curve established. Mann-Whitney test. The estimated mean PFU per million platelets is shown in blue, with 95% confidence intervals.

E) Scheme of the experiments evaluating platelet-mediated SARS-CoV-2 trans-infection of macrophages *in vitro*. SARS-CoV-2 -containing platelets from non-survivors interacted with macrophages in the presence or absence of abciximab (anti-GpIIbIIIa) for 2 hours (pulse) followed by 24-hour chase. At these time-points, macrophages positive for (+) and (-) SARS-CoV-2 RNA were assessed by *in situ* hybridization and macrophage supernatants were collected and further evaluated for infectious virus content in reporter Vero cells. SARS-CoV-2 RNA^+/$dsRNA^+$ Vero cells were assessed by *in situ* hybridization and quantified by FISH-flow.

F) Confocal microscopy images of SARS-CoV-2 RNA *in situ* hybridization (red) for positive (+) and negative (-) strand RNA in macrophages that interacted *in vitro* with platelets samples from COVID-19 non-survivors. Images were acquired after 2 hours of interaction with platelets (pulse, left) or 24 hours after interaction (chase, right). Images show three-dimensional projections (xy, xz and yz, bar=10μm). Arrowheads indicate SARS-CoV-2 RNA. Macrophage nuclei are stained with DAPI (blue).

G) Outgrowth in Vero cells of SARS-CoV-2 produced by macrophages after platelet-mediated infection. On the left, confocal microscopy image of double-strand RNA (dsRNA, red) in Vero cells cultivated with macrophage supernatants for 24 hours. Arrowheads indicate infected Vero cells (bar=30μm), Vero cells nuclei are stained with DAPI (blue). On the middle graph, the number of infected Vero cells were quantified by FISH-flow and expressed as % of SARS-CoV-2 RNA^+/$dsRNA^+$ Vero cells, comparing negative controls (medium, gray=non-infected Vero), positive controls (virus, green=primary SARS-CoV-2 obtained from patient bronchoalveolar lavage) and COVID-19 non-survivors platelets after pulse (2 hours interaction with macrophages, light red) and chase (24 hours after interaction with macrophages, red). Asterisk indicates statistical significance in the comparison between pulse and chase (Mann-Whitney). The right graph shows the outgrowth of SARS-CoV-2 in Vero cells incubated with macrophages that interacted with COVID-19 non-survivors' platelets in the presence or not of abciximab (10μg/ml) also quantified by FISH-Flow. Results are expressed as % of SARS-CoV-2 RNA^+/$dsRNA^+$ Vero cells in the two conditions. The % inhibition of Vero cell infection in the presence of abciximab is indicated with asterisk corresponding to statistical significance in the comparison between the two groups (Student T-test).

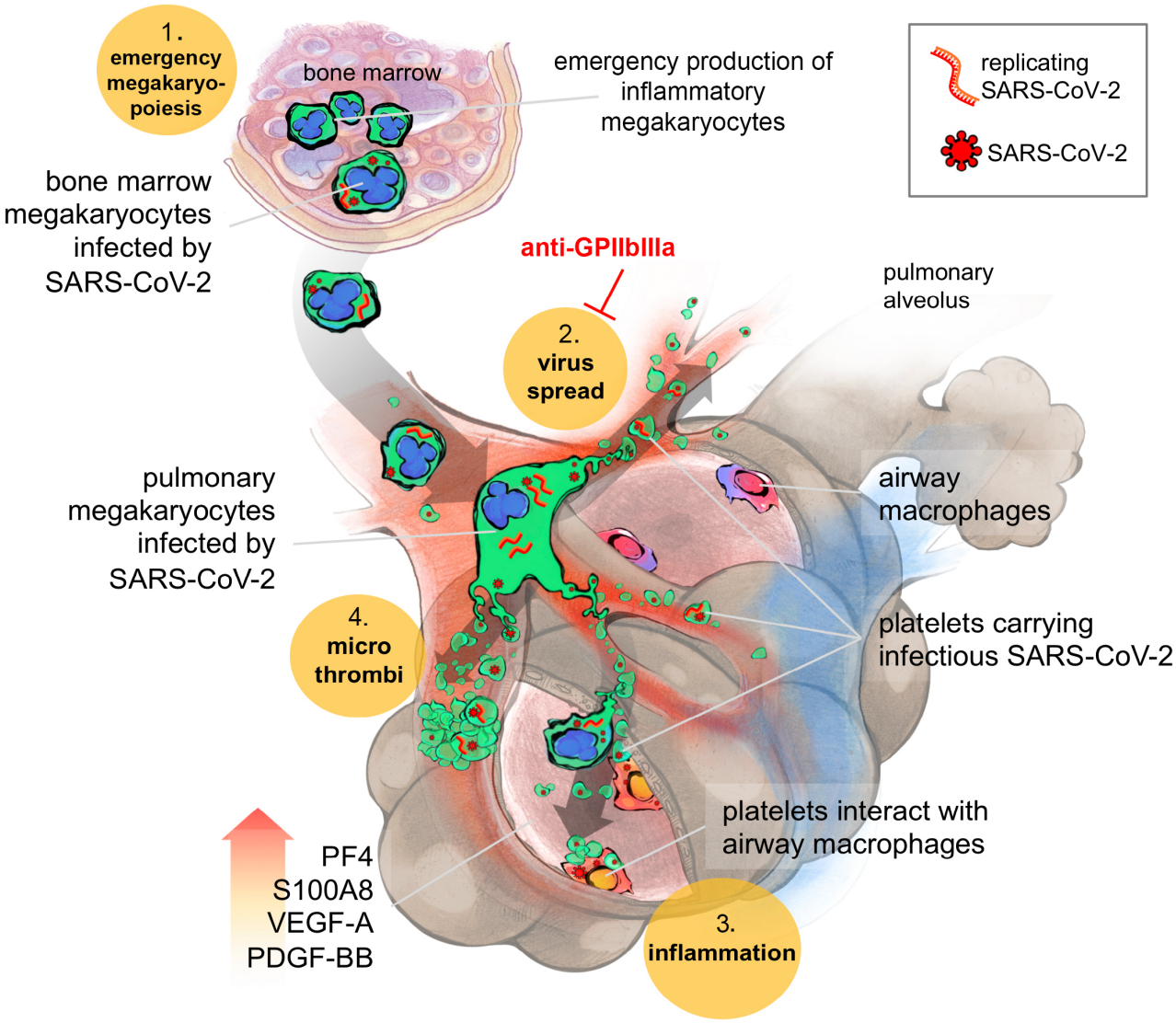

Figure 5: Scheme: Platelets harboring SARS-CoV-2 offer a convergent therapeutical target in severe COVID-19 with multiple manifestations.

1- SARS-CoV-2 favors emergency inflammatory megakaryopoiesis. SARS-CoV-2 infected MKs in the bone marrow (containing both viruses and replicating SARS-CoV-2 (-) RNA) migrate to the lungs where they contribute to thrombopoiesis, and produce SARS-CoV-2-containing platelets in the pulmonary circulation.

2- These infectious platelets will then spread the virus and contribute to the systemic inflammatory component of severe COVID-19. As platelets sheltering SARS-CoV-2 are coated with Von Willebrand Factor, indicating their highly activated status, they will also contribute to thrombus formation typical of COVID-19 complications.

3- Increase in lung VEGF-A and PDGF-BB participates to alveolar endothelial destruction and effraction allowing for platelets carrying SARS-CoV-2 to reach and infect alveolar macrophages.

4- Increased lung PF4 released by platelets and S100A8 likely contributes to the maintenance of a highly inflammatory environment, macrophage activation, and cytokine storm.

These three platelet-mediated components of severe COVID-19 suggest that targeting platelets, with the use of anti-platelet drugs like anti-GPIIbIIIa, might be an efficient strategy to block viral spread, thrombus formation and exacerbated inflammation at once, increasing the chance of survival.

Tables

Table 1: **Patient characteristics according to the hospital outcome (PRP samples)**

Median [IQR]; N(%)	**Survivors, n=27**	**Non-survivors, n=25**	***p*-value**
Patients			
Age, years	61.6 [52.0;76.2]	72.7 [68.4;87.9]	**0.009**
Male sex	17 (63%)	16 (64%)	1.00
At least one comorbidity	22 (81%)	23 (92%)	0.42
Obesity	6 (19%)	2 (8%)	0.27
High Blood pressure	8 (30%)	10 (40%)	0.56
Cardiovascular disease	7 (26%)	8 (32%)	0.76
Diabetes	6 (22%)	10 (40%)	0.23
Active malignancy	5 (19%)	5 (20%)	1.00
Chronic renal failure	1 (4%)	2 (8%)	0.60
Chronic respiratory failure	4 (15%)	3 (12%)	1.00
At Hospital admission			
Days since first symptoms	10 [6.5;25.5]	8 [5;12.5]	0.23
Need of oxygen supply	2 (7%)	5 (20%)	0.24
O2 saturation, %	91 [88;98]	91.5 [82;95.75]	0.40
ICU admission	11 (41%)	12 (48%)	0.78
IGSII*	32 [30;39]	45 [34.25;57]	0.16
SOFA*	4 [3; 5]	4 [3.75; 8.75]	0.49
At Sampling time			
Days since first symptoms	10 [6;26]	7 [5;12.5]	0.22
WBC count, Giga/L	7.4 [5.3;9.65]	9.2 [6.4;13.8]	0.26
Platelet count, Giga/L	238 [138.5; 334]	189 [160;255]	0.40
Fibrinogen in plasma, g/L	6.5 [5.175;7.525]	6.6 [4.9;8.1]	0.72
D-dimer in plasma, mg/L	4.4 [2.5;5.6]	3.5 [1.2;4.3]	0.091
vWF in plasma, μg/ml**	9.6 [7.448;14.35]	18.0 [12.56;27.33]	**0.015**
%vWF^{+} platelets**	5.9 [3.6;7.8]	14.5 [8.6;19.5]	**0.001**
SARS-CoV-2 in platelets	1 (4%)	19 (76%)	**<0.0001**
At Hospital discharge			
Days from first symptoms to discharge	25 [18;72]	15 [12.5;28]	**0.01**
Days from sampling to discharge	13 [10;44]	7 [5;10]	**0.001**

*only available in those patients admitted to ICU (11 survivors and 12 deceased patients)
** only measured in 16 survivors and 14 non-survivor patients

Table 2: **Patient characteristics according to the hospital outcome (autopsy samples)**

Patient	Sex	Age	Sample Origin	ICU days	Days until demise	BMI index	Cardio Vascular	Pre-existing condition	Treatment	Cause of death	Lung sampling	Bone Marrow sampling
A1	F	82	France	11	17	24.1	0	N.A.	N.A.	Multivisceral failure	Yes	Yes
A2	M	51	France	10	20	34.5	AHT, AVB1	Small airways obstruction/ Leukemia	AINS	Pulmonary embolism	Yes	No
A3	F	59	France	13	18	28.4	AHT	Asthma	Corticoids	Pulmonary embolism	Yes	Yes
A4	M	51	France	11	19	38	AHT	Small airways obstruction/ Arthritis	N.A.	Massive Pulmonary embolism	Yes	Yes
A5	M	71	France	0	N.A.	N.A.	Low grade coronary illness	Marked hepatic steatosis	N.A.	major pulmonary edema	Yes	No

Abbreviations: COVID-19: Coronavirus disease 19; LC: Lung Carcinoma; TB: tuberculosis; N.A.: not applicable; N/R: not register; F: Female; M: Male; AINS: non-steroidal anti-inflammatory drugs. AHT: Arterial Hypertension), AVB1: Atrioventricular block level 1.

Table 3: **Patient characteristics according to the hospital outcome (BAL samples)**

Median [IQR]; N(%)	**Survivors, n=6**	**Non-survivors, n=13**	***p*-value**
Patients			
Age, years	54 [42;66]	69 [63;77]	**0.046**
Male sex	5 out of 6 (83%)	7 out of 13 (53%)	0.33
At least one comorbidity*	5 out of 6 (83%)	5 out of 11 (45%)	0.62
Obesity*	1 out of 6 (16%)	1 out of 11 (9%)	1.00
Cardiovascular disease*	2 out of 6 (33%)	4 out of 11 (36%)	1.00
Diabetes*	2 out of 6 (33%)	2 out of 11 (18%)	0.58
At Hospital admission			
Days since first symptoms*	9 [6;9]	4.5 [3;7]	0.49
PPP	1 [1;4.5]	1 [1;1.5]	0.83
ICU admission	6 out of 6 (100%)	13 out of 13 (100%)	-
Need of oxygen supply at ICU admission*	5 out of 6 (83%)	10 out of 12 (83%)	1.00
At Sampling time			
SARS-CoV-2 in BAL fluid	4 out 6 (66%)	6 out 13 (46%)	0.62
At Hospital discharge			
Days from first symptoms to discharge*	46.5 [38.5;66]	41.5 [23;51.5]	0.57
Days from sampling to discharge*	21 [20;74]	25 [12;27]	0.89

*only available indicated number of patients